



Published in final edited form as:

*Bone*. 2012 August ; 51(2): 224–231. doi:10.1016/j.bone.2011.11.012.

## Serum Xylosyltransferase 1 Level Increases during Early Posttraumatic Osteoarthritis in Mice with High Bone Forming Potential

Sarah Y. McCoy, Kerry A. Falgowski, Padma P. Srinivasan, William R. Thompson, Erica M. Selva, and Catherine B. Kirn-Safran<sup>†</sup>

University of Delaware, Department of Biological Sciences, Newark, DE

### Abstract

Increased proteoglycan (PG) synthesis is essential for the stimulation of cartilage repair processes that take place during the reversible phase of osteoarthritis (OA). In articular cartilage, xylosyltransferase 1 (Xylt1) is the key enzyme that initiates glycosaminoglycan (GAG) chain synthesis by transferring the first sugar residue to the PG core protein. Biological activity of PGs is closely linked to GAG biosynthesis since their polyanionic nature directly contributes to the proper hydration and elastic properties of the cartilage tissue present at the articular interface. The aim of this study was to investigate whether variations in the level of Xylt1 present in serum can be used to predict OA disease progression. The influence of bone forming activity on the systemic release of this enzyme was addressed by experimentally-inducing OA in mice of two different genetic backgrounds that were previously characterized for their distinct bone metabolism: C57BL/6J (B6, high bone remodelers) or C3H/HeJ (C3H, high bone formers). Serum was collected after medial meniscectomy or sham surgeries in young adult mice of these two strains over a period of 3.5 months at which point knee histopathology was assessed. A significant increase in serum Xylt1 levels observed shortly after meniscectomy positively correlated with severe cartilage damage evaluated by histological assessment at later time points in mice of the C3H background. In contrast, no temporal regulation of Xylt1 level was found between meniscectomies and control surgeries in B6 mice, which developed OA at a slower rate. Additionally, longitudinal evaluation of the serum levels of other markers of cartilage/bone metabolism (C1,2C, osteocalcin) did not reveal any association with late knee damages. Our results strongly support the idea that serum Xylt1 has a clinical value for monitoring risk of OA progression in young adults with high bone forming potential. Ultimately, the understanding of posttraumatic mechanisms regulating PG synthesis and their modification by GAG will be essential so that interventions that stimulate cartilage regrowth can be undertaken prior to irreversible destruction of the joint tissue.

### Keywords

Cartilage; Osteoarthritis; Biomarkers; Xylosyltransferase; Longitudinal Study

---

© 2011 Elsevier Inc. All rights reserved.

<sup>†</sup>Author to whom correspondence should be addressed: Catherine Kirn-Safran, University of Delaware, Department of Biological Sciences, 310 Wolf Hall, Newark, DE 19716, Telephone: (302) 831-3249, Telefax: (302) 831-2281, ckirn@udel.edu.

**Publisher's Disclaimer:** This is a PDF file of an unedited manuscript that has been accepted for publication. As a service to our customers we are providing this early version of the manuscript. The manuscript will undergo copyediting, typesetting, and review of the resulting proof before it is published in its final citable form. Please note that during the production process errors may be discovered which could affect the content, and all legal disclaimers that apply to the journal pertain.

## Introduction

Osteoarthritis (OA) is a complex, progressive disorder characterized by articular cartilage loss and changes in joint structures including joint space narrowing, osteophyte formation and ligament laxity. Knee OA is more commonly known as a degenerative disorder in the population over the age of 65, however, it does arise in the younger population from overuse and trauma. Posttraumatic OA is thought to account for approximately 12% of the total cases of symptomatic OA in the United States and can be modeled in mice by surgically inducing joint instability [1–4]. In such models, OA develops rapidly and joint changes occurring in the early, reversible phase of OA can be studied longitudinally in a relatively short period of time.

The presence of highly negatively charged extracellular matrix (ECM) components in articular cartilage allows this highly specialized tissue to retain hydration and to resist mechanical load. OA is believed to develop from an imbalance between synthesis and degradation of both cartilage and subchondral bone ECM molecules that eventually lead to a loss of cartilage function [5]. Biomarkers of cartilage and bone ECM synthesis or degradation detected in body fluids (synovial fluid, blood, and urine) can serve as valuable tools to assess changes in matrix turnover and can be indicative of a specific disease state. However, to date only a few useful biomarkers have been identified that can be used as early stage OA indicators. The two main structural components of articular cartilage ECM are type II collagen fibrils and the proteoglycan (PG) aggrecan. During OA progression, several proteases are activated which cleave type II collagen revealing neo-epitopes that are markers of collagen degradation. For example, cleavage products of collagen fibril degradation generates neo-epitopes such as C1,2C (also known as Col2-3/4C short fragment), which are cleared in the peripheral blood and can be measured in serum as indicators of collagen break-down and progressive joint destruction [6,7].

During the initial phase of OA, cartilage damage can also induce *de novo* synthesis of matrix components in order to compensate for loss. Such markers of synthesis include amino- and carboxy-terminal propeptide of type II procollagens, PG core proteins, and sulfated glycosaminoglycans (GAG) [8,9]. Besides the appearance of a chondroitin sulfate neopeptide (CS846) on newly synthesized aggrecan, the synthesis and assembly of GAG chains on PGs have received little attention in OA research. Yet, the presence of GAG chains with negatively charged sulfate groups on PGs such as aggrecan is absolutely essential for providing proper compressive strength to the joint tissue. The initial step that transfers one D-xylose from UDPD-xylose to specific serine residues of the core protein and initiates all GAG (chondroitin and heparan sulfate) chain elongation is catalyzed by xylosyltransferases. During cartilage development, this rate-limiting step is controlled by the xylosyltransferase 1 (Xylt1) isoform which is also implicated in the early phase of cartilage repair during reversible OA [10,11]. Recently, Xylt activity in the serum was found to be increased during sclerotic disease processes and proposed to be a biomarker for the rate of PG biosynthesis [12]. In addition, mutations in *XYLT* genes were potentially linked with early manifestation of OA [13].

The goals of the current study were to investigate whether the appearance in the circulation of the soluble form of Xylt1 can be used as a biomarker to predict onset of posttraumatic OA and to define the importance of bone forming potential on the release of this enzyme during the reversible phase of the disease. For this purpose, we performed medial meniscectomy in two strains of mice (C57BL/6J: B6 and C3H/HeJ: C3H) with distinct bone metabolism [14] at a young age, and measured longitudinal changes in the serum levels of Xylt1 and two established biomarkers of collagen degradation and bone synthesis. Interestingly, a

significant increase in serum Xylt1 levels was only detected during the early stages of OA development in the strain that exhibits higher bone forming activity and peak density (C3H).

## Material and Methods

### Experimental Animal Model

Ten to eleven week-old C57BL/6J (B6) and C3H/HeJ healthy male mice were used in this study (n = 5/group except for animals sacrificed at 1 month post-surgery where n=4). Experimental OA was surgically induced by medial MNX using an adaptation of the destabilization of the medial meniscus (DMM) method described by Glasson et al. [2]. All knee surgeries were performed on the right knee under anesthesia by mask inhalation with 1.5–2% isoflurane. A three mm incision was made proximal to the tibial plateau, and the joint capsule was incised medially to the patellar tendon. Dissection of the fat pad was performed to visualize the intercondylar notch of the knee. Occasional mild hemorrhage was controlled with cotton swabs. The meniscotibial ligament anchoring the medial meniscus to the tibia was transected with micro-surgery scissors and the medial meniscus was partially dissected out. The joint capsule was closed with three absorbable 8-0 Vicryl sutures (Ethicon, Somerville, NJ) and the skin was closed with a drop of surgical tissue adhesive (GLUture, Abbott Labs, Abbott Park, IL). This model simulates posttraumatic OA by increasing mechanical stress on the medial femur and tibia and accelerates disease progression when compared to the milder DMM model [2]. Sham surgeries consisted of knee arthrotomies without ligament transection and meniscus removal. After surgery, mice were housed in individual cages, fed normal diet and tap water, and euthanized 3.5 months later for longitudinal biomarker studies. The end point of this study was selected based on preliminary work performed in C57BL/6J mice that showed articular cartilage defects equivalent to early to mid stage OA 3.5 months post-operatively. Assessment of knee histology was conducted at additional time points including 1, 2, and 5 months post-surgery. All procedures involving animals were performed in accordance with protocols approved by the IACUC at the University of Delaware.

### Blood Sample Collection

Up to 500µl of blood was collected via retro-orbital bleed as early as seven days post-surgery and as often as every 14 days thereafter. The samples were allowed to clot at room temperature for 10–15 min and stored on ice. Following a 15 min centrifugation at 3000 rpm, the supernatant was collected and spun again for another 15 min at the same speed. Protease inhibitors (1:100) were added to serum samples prior to storage at –80°C.

### Cartilage Histological Assessment

Whole knee joints (n = 5/group except for histology at 1 month post-surgery where n=4) were dissected and fixed with 10% formalin (v/v) for 24 hr and decalcified in 10% (v/v) formic acid in PBS over seven days on a rocking platform. The formic acid solution was changed each day. The joints were embedded in paraffin and 6µm-thick frontal sections were obtained through the entire joint. After deparaffinization, the sections were stained using a standard Safranin O and Fast Green staining procedure [15].

Knee sections were scored following the OARSI histopathology grading system as described [16]. Briefly, mean scores were obtained for all four knee compartments; medial tibia (MT), medial femur (MF), lateral tibia (LT), and lateral femur (LF). A grade score (0–6) was assigned for the severity of damage and a stage score (0–4) was given for the extent of damage over the joint surface, a combined score was calculated by multiplying the grade by the stage. For each knee analyzed, 24–30 coronal sections encompassing around 400µm were scored using the two femoral growth plate half circles as a central reference point

(Supp. Fig. 1). This region corresponds to the joint area where the meniscus was removed. Blinded sections were scored by two independent observers.

### SDS PAGE and Western Blotting

Serum Xylt1 levels were analyzed by Western Blotting. All surgery samples were run alongside samples from the same time point and each gel was run in duplicate. A pooled serum sample obtained from ten young skeletally immature B6 mice (10 week-old) that were not subjected to surgery was aliquoted and stored at  $-80^{\circ}\text{C}$  to serve as an internal load control. This sample was run on all gels and used to normalize densitometric values across the entire study (Supp. Fig. 2). Serum samples were diluted in PBS by adding 2  $\mu\text{l}$  of serum to 5  $\mu\text{l}$  of PBS and were diluted in Laemmli sample buffer in  $\beta$ -mercaptoethanol and denatured at  $95^{\circ}\text{C}$  for 8 min. Prepared samples were loaded on precast 7.5% SDS polyacrylamide gels using the BioRad mini-protean TGX system (Hercules, CA). Gels were run for 1.5 hr at 100 V. Following electrophoresis, gels were transferred to a polyvinylidene fluoride (PVDF) membrane using a semi-dry transfer apparatus for 35 min at 10 V. The blots were blocked in 5% (w/v) milk in Tris-buffered saline-Tween 20 (TBS-T) overnight at  $4^{\circ}\text{C}$  on a shaker, then incubated for 2 hr at room temperature in  $\alpha$ -Xylt1 antibody at a 1:1,000 dilution (Sigma-Aldrich, St. Louis, MO; HPA007478) in 5% (w/v) milk in TBS-T. This antibody is directed against an isoform-specific carboxy terminal peptide of Xylt1 and recognizes both membrane-bound and shed forms of this enzyme. The blots were washed 3 times for 10 min each in TBS-T, and incubated for 1 hr at room temperature with a horseradish peroxidase-conjugated  $\alpha$ -rabbit IgG (Jackson ImmunoResearch Laboratories, Inc., West Grove, PA) at a 1:10,000 dilution. Following 3 washes of 20 min each in TBS-T, detection was performed using the SuperSignal West Dura Chemiluminescent Substrate Pierce detection kit (Thermo Fisher Scientific, Rockford, IL). Densitometry analysis was performed using Image J<sup>®</sup> software (NIH, Bethesda, MD). Each serum sample was run on two independent western blots along with the serum sample that served as an internal control and the average of ten normalized densitometric values (five animals per group) were plotted for each individual time point (six bleeds per animal between 1 and 3.5 months post-surgery).

### C1,2C and Osteocalcin ELISA assays

Markers of collagen and bone metabolism were measured by enzyme linked immunosorbent assay (ELISA). Appearance of the C1,2C neo-epitope which corresponds to an 8 amino acid sequence on the carboxy terminal fragment of the three-quarter length fragment generated by collagenase cleavage of type II collagen was measured by an ELISA assay that utilizes a rabbit antibody (IBEX Diagnostics, Montreal, Québec, Canada). Because the C1,2C antibody also reacts with similarly cleaved type I collagen chains, C1,2C levels reflect turnover of both cartilage and bone. Osteocalcin concentrations were determined using a sandwich ELISA assay specific for intact mouse osteocalcin (Biomedical Technologies Inc., Stoughton, MA). All samples were run in duplicate (C1,2C) or triplicate (osteocalcin) on plates from the same lot and were analyzed by a four parameter logistic equation generated by MasterPlex<sup>®</sup> EX software (San Francisco, CA).

### Statistical Analyses

Results are reported as mean  $\pm$  standard deviation for five animals per experimental group (sham vs. surgery) unless otherwise stated. The histological scores were analyzed using the Kruskal-Wallis statistical test followed by a Bonferroni correction for multiple comparisons and p values less than 0.0125 were considered significant (four groups for scores within or between mouse strains). For Xylt1 and osteocalcin analyses, statistical comparisons between surgery and sham controls were performed using a two-tailed Student's t-test at specific time points and p values less than 0.05 were considered significant. Associations between

histological scores and Xylt 1 levels were made using a linear regression method. One-way ANOVA followed by Tukey-Kramer post-hoc test was used to compare C1,2C values at different time points. Analyses were performed using a statistical package software provided by Dr. John H. McDonald (University of Delaware, Newark, DE) as described [17].

## Results

### 1. Posttraumatic OA Progression in B6 and C3H inbred strains

**1.1 Effect of MNX on B6 knees**—Histological analysis of meniscectomized (MNX) B6 knees demonstrated progressive expansion of focal articular cartilage loss at their medial side between 2 and 3.5 months post - surgery (compare panel C and E in Fig. 1). At five months post-surgery, complete cartilage loss was accompanied by the absence of obvious bone marrow space in bone present at the medial tibio-femoral junction indicating abnormal turnover in favor of excessive bone synthesis (see asterisks, in Fig. 2C MNX and compare medial to lateral sides in Fig. 2G). This was reflected by a significant increase of mean histological scores at the MNX medial side for both tibial (MT) and femoral (MF) joint surfaces compared with medial surfaces in sham control knees (compare MF+MT<sub>MNX</sub> vs. MF+MT<sub>sham</sub> in Fig. 2A, \* $P<0.0125$ ). Although, the lateral tibial plateau (LT) and lateral femoral condyle (LF) surfaces of the MNX-operated knee contained fewer cartilage lesions their scores remained significantly different from sham controls (LF+LT<sub>MNX</sub> vs. LF+LT<sub>sham</sub> \* $P<0.0125$  in Fig. 2A). Additionally, a significant difference was also found between medial to lateral scores of the meniscectomized knee (Fig. 2A, MT+MF<sub>MNX</sub> vs. LT+LF<sub>MNX</sub>, # $P<0.0125$ ).

**1.2. Histopathological evaluation in B6 versus C3H**—Analysis of B6 and C3H meniscectomized knees at 3.5 months revealed a clear difference in the extent of cartilage damage (compare Fig. 1E to Fig. 2C MNX). Indeed, full-thickness loss of articular cartilage associated with increased subchondral bone density was observed on the medial side of the operated knee in C3H mice at 3.5 months (Fig. 2E and H) whereas identical cartilage damage was only observed 5 months following surgery in B6 mice (Fig. 2C and G). In contrast, B6 medial articular surfaces only showed cartilage breakdown characteristic of mid-stage OA with superficial cartilage delamination at 3.5 months post-surgery (Fig. 1E). Medial histological scores obtained in meniscectomized knees were indistinguishable between C3H at 3.5 months and B6 at 5 months (MF+MT<sub>MNX</sub> B6 vs. MF+MT<sub>MNX</sub> C3H:  $P=0.65$ ). Within each strain, medial scores were significantly different between MNX (Fig. 2C, E, G, and H) and sham (Fig. 2D, F, I, and J) surgeries (compare MT+MF<sub>MNX</sub> vs. MT+MF<sub>sham</sub>,  $P<0.0125$  in Fig. 2A or Fig. 2B).

### 2. Longitudinal analysis of circulating biomarker levels and correlation with histological assessment

**2.1. Marker of proteoglycan synthesis and maturation: Xylt1**—In MNX B6 mice where complete articular cartilage deterioration was observed 5-months post-surgery in the operated knee, no change was observed in the circulating levels of the shed form of Xylt1 and its relative amount remained identical to the levels found in sham animals during the first 3.5 months following surgery (Fig. 3A). In contrast, a transient and significant increase of Xylt1 levels was observed at 1.5–2 months post-surgery in MNX C3H mice when compared to sham C3H at the same time points (Fig. 3B and Supp. Fig. 2, \* $P<0.005$ ). This increase was followed by a decrease to sham levels at 2.5 months (Supp. Fig. 2); then a second rise in the Xylt1 levels was observed at 3.5 months in MNX C3H relative to strain-matched sham controls. This second increase in Xylt1 levels was not associated with damages in non-operated contralateral knees but may coincide with initiation of damages in the lateral compartment of the operated knee (Fig. 2J, and Supp. Fig. 3). Statistical analysis



showed that Xylt1 serum levels in the C3H can differentiate meniscectomized versus non-injured sham animals (Fig. 3B). A positive correlation between Xylt1 levels and histological medial end scores of meniscectomized knee was found in C3H mice at the 2-month post-operative time point (Fig. 4B,  $r^2=0.4645$ ,  $P=0.043$ ). In contrast, a non-significant correlation was found between Xylt1 levels and histological scores in B6 mice at all post-operative time points (Fig. 4A).

**2.2. Marker of collagen degradation: C1,2C neoepitope**—Longitudinal assessment of the appearance of collagenase-induced degradation fragments in serum following surgery did not reveal differences between MNX and sham animals in both B6 and C3H strains (Fig. 5). However, two distinct patterns were seen in C3H vs. B6 mice. With C3H mice, C1,2C levels were significantly higher (Fig. 5B,  $\sim 0.35\mu\text{g/ml}$ ) at the beginning of the longitudinal study (1 month post-operatively or 14 weeks of age) and decreased and remained stable once skeletal maturity was reached after 16 weeks of age. In contrast, C1,2C levels spiked later in B6 mice and increase roughly two-fold at 22 weeks (Fig. 5A, 3 months post-operatively;  $\sim 0.25\mu\text{g/ml}$ ) relative to earlier post-operative (1–2 months) time points in both MNX and sham controls. In both strains, the concentration of C1,2C stabilized by the time the study ended (24 weeks). Interestingly, a local increase in the immune signal specific for this C1,2C neoepitope was observed in articular cartilage regions displaying early signs of damage (proteoglycan depletion and small surface fibrillation) and located near areas with higher damage in MNX mice of both the B6 and C3H backgrounds (Supp. Fig. 4). In contrast, the weaker C1,2C signal detected in sham controls remained unchanged throughout the intact articular cartilage tissue (Supp. Fig. 4). Although local changes in the  $\frac{3}{4}$  collagen II fragment were detectable following MNX, no correlation was found between C1,2C levels circulating in the blood and histological scores.

**2.3. Marker of bone synthesis: Osteocalcin**—Serum osteocalcin was significantly higher in B6 mice compared with that of C3H mice at 0.5 (51%,  $P<0.01$ ), 2.5 (56%,  $P<0.01$ ), 3.5 months (45%,  $P=0.01$ ) post-surgery in sham controls whereas the difference was only significant at 2.5 months (42%,  $P<0.05$ ) in MNX animals. Osteocalcin levels were high at the beginning of the study and decreased steadily over time in both sham and MNX animals (Fig. 6). While a small increase in osteocalcin is seen in MNX vs. sham at 1.5 months in both strains, this change was not significant ( $P=0.088$  in B6, and  $P=0.276$  in C3H). Osteocalcin levels are not statistically different between C3H and B6 mice at 1.5 months post-surgery. Interestingly, this time point also corresponds to skeletal maturity for these animals (16 week-old).

In summary, we observed significantly higher levels of Xylt1 at early time points following surgery and association with end scores in the serum of C3H mice, while only a small trend was seen for osteocalcin when sham surgeries and meniscectomies were compared. In contrast, time (associated to the animal cartilage/bone remodeling) influenced C1,2C levels, but not the knee destabilization procedure in either strain.

## Discussion

In the current study, we investigated the association of knee articular cartilage damage with serum Xylt1 levels in a longitudinal study using the meniscectomy model of posttraumatic OA in mice. To our knowledge, this is the first report evaluating Xylt1 as a biomarker to predict OA disease progression. Novel circulating biomarkers are needed to identify disease activity prior to severe radiographic changes [18]. Previously, up-regulation of Xylt1 expression was found to be associated with cartilage repair activity in models of reversible OA [10]. Additionally, the soluble active form of Xylt1 was found to be increased in serum samples of patients with abnormally high PG biosynthetic rates [12]. Thus, we hypothesized

that increased detection of soluble forms of Xylt1 in serological samples of animals experimentally induced to develop OA constitutes an early molecular event of cartilage degradation.

This study involved two inbred mouse strains with different bone formation and mineral accrual rates that responded distinctly to surgically-induced OA. Faster OA progression in C3H is likely due to a higher rate of subchondral bone formation in young C3H animals relative to age-matched B6 mice that results in higher peak bone density [14,19,20]. The contribution of subchondral bone properties to OA progression has been previously examined and longitudinal studies indicate that elevated bone mineral density (BMD) may be an important predictor of knee OA [21]. Additionally, patients diagnosed with OA show increased subchondral BMD at osteoarthritic sites associated with osteophytes, decreased joint space, and positive bone scintigraphy [22–24]. Thus, it has long been thought that abnormal metabolic activity of osteoblasts in subchondral bone plays a key role in the initiation and progression of OA [25]. Here, our data suggest that the high bone forming activity of young C3H mice is a determining factor for increasing OA onset. Although OA progressed at a slower rate in B6 mice, skeletal changes were also detected and are believed to be due to rapid bone turnover in response to altered joint loading [26,27].

Although chondrocytes can also respond to mechanical load, their capacity to repair the surrounding extracellular matrix is limited when compared to osteoblasts, particularly following acute injuries that alter joint mechanics [28]. Here, we show that elevation of serum Xylt1 occurs rapidly following meniscectomy in a strain of mice with high bone forming activity and fast OA progression. It is unclear why increased levels of Xylt1 are only observed in rapid progressors with high bone activity. However, we can speculate that a shorter window of disease progression will result in increased concentrations of Xylt1 in the serum. With regard to elevated Xylt1 levels during active bone formation, recent reports consistent with our current finding showed that bone deposition and mineralization are associated with increased soluble Xylt1 enzymatic activity both *in vitro* and *in vivo* during active skeletal growth in children [29,30]. In joint tissue, it has long been known that initial acute injury is accompanied by a wave of PG and sulfated GAG synthesis that occurs during the reversible phase of OA before degradation of the collagen fibrillar meshwork [31]. Similarly to Xylt1, transient increase in CS486, a neoepitope found on chondroitin sulfate chains of newly formed aggrecan molecules and detected during cartilage growth and repair, was measured in synovial fluid and serum during the early phase of equine OA [9,32]. Another recent study demonstrated a significant increase in sulfated proteoglycan levels after acute ACL injury in synovial fluid of patients [33]. Our present study is also comparable to a recent longitudinal biomarker study performed in cadets at the US Military Academy treated with ACL reconstruction that demonstrated increase in serum CS846 levels in early arthritic joints [34]. In this report, a second increase in Xylt1 levels was observed in C3H sera at the end of the study when full-thickness loss of articular cartilage was already attained in the operated knee. Although this increase did not reach significance when compared with sham controls, it is tempting to hypothesize that this second round of release in the serum corresponds to the initiation of degradation processes in the lateral compartment of the operated knee. Partial medial MNX induces aberrant walking patterns that are implicated in the activation of degradative pathways. Typically, in unilateral OA mouse models, lesions occur first at the medial compartment and progress to the lateral side of the operated knee and under some circumstances (altered genetic background) may even progress relatively rapidly to the lateral compartment of the non-operated knee [35]. Under our experimental conditions, mild degradative damages started to be visible only on the lateral side of the operated knee and longer post-operative periods will be required to determine whether OA progresses to the non-operated side.

One disadvantage of conducting longitudinal biomarker studies in mice is the fact that no commercial mouse-specific assay exists for assessment of cartilage matrix turnover biomarkers. Hence, the current study used Western blot analysis to monitor circulating levels of Xylt1 and relied on a load control for inter-assay reliability. Xylt activity was found in the early Golgi compartments where its primary function is to modify PGs intracellularly [36]. The mechanisms regulating xylosyltransferase presence in the extracellular milieu are currently not completely understood. In cartilage, it is unknown whether Xylt1 is transported at the cell surface in matrix vesicles and then cleaved via the action of specific metalloproteinases/sheddases or if it is simply secreted simultaneously into the extracellular space with chondroitin sulfate or heparan sulfate PGs [12,37]. Future work will consist of designing a more sensitive assay that will detect soluble forms of Xylt1 in both cartilage explant secretions and body fluids and will be able to distinguish between enzymatically active and non-active isoforms.

In addition to Xylt1, we used an ELISA assay originally designed for detection of a degradation neopeptide of human collagen but cross-reacting with murine collagen fragments to monitor joint matrix degradation following knee destabilization. While the presence of the C1,2C neopeptide provided direct evidence of enhanced collagen degradation in the vicinity of severe OA lesions and was found by others to show rapid clearance from the joint following acute knee trauma [33], our study did not reveal significant changes between MNX and sham controls for this biomarker in serum, which may reflect the limitation of our study design to detect transient systemic changes. Although mouse models allowed us to study posttraumatic OA progression on fixed genetic backgrounds, one of the limitations of using mice is that only limited blood volumes can be collected from the same individual every other week, thus, preventing large comparative longitudinal studies between multiple markers in time-matched samples. Nonetheless, significant differences in the concentration of C1,2C were found within strains between the analyzed time points. Elevated levels of C1,2C in C3H mice are believed to be due to high collagen turnover at time preceding skeletal maturity [14]. Conversely, elevated C1,2C levels in skeletally mature B6 mice is consistent with the high bone remodeling potential of this strain during adulthood. Unfortunately, such systemic changes in collagen metabolism impair detection of rapid local changes occurring at the site of injury and associated with increased subchondral bone turnover and cartilage degradation.

Serum osteocalcin concentrations were analyzed as a marker of bone turnover in this study. A significant increase in both synovial fluid and serum osteocalcin levels was reported in early OA-affected horses [32]. Recent data investigating osteocalcin levels following acute ACL trauma in eleven patients suggested a knee source for osteocalcin and the ability of osteocalcin serum level to reflect early knee damage events after injury [33]. Despite these reports in other species and a small increase in the level of osteocalcin during the early post-operative period, we did not find significant differences in osteocalcin concentrations between MNX and sham control animals. Thus, changes in osteocalcin levels reflected primarily changes in global bone metabolism rather than more subtle and hard to detect events associated with an anabolic response of subchondral bone in MNX knees. Because osteocalcin levels are known to be significantly increased in synovial fluid and serum following the onset of exercise, it is possible that significance between sham and control surgeries may have been reached if knees were subjected to load following surgery, particularly in the B6 strain which displays an enhanced bone formation response to load relative to C3H [27,32,38]. In agreement with our data, two studies showed no strong association between osteocalcin levels and the presence of OA symptoms in large patient cohorts that were not subjected to specific physical activity programs [39,40]. Our finding of lower amounts of osteocalcin in C3H serum compared with B6 serum reflects differences in bone metabolism in these two strains and is consistent with previous work performed in age-



comparable mice [41]. In this study, the authors proposed that the variation in osteocalcin concentrations may be due to a smaller release of synthesized osteocalcin into the extracellular fluid in C3H mice when compared with B6 mice. Since it is well established that C3H mice are high bone formers, lower concentrations of osteocalcin in these mice is in direct contradiction with the idea that levels of osteocalcin directly reflect bone formation activity and strongly suggests that additional factors control the systemic release of osteocalcin into peripheral blood.

Due to the complexity of the mechanisms involved in the regulation of molecules associated with mineral bone accrual and bone turnover in the blood, we would not recommend the use of either osteocalcin or C1,2C as biomarkers for the early detection of osteoarthritic lesions in young adults with high bone forming and remodeling potentials. Based on this study, determination of Xylt1 levels in serum samples may constitute a more appropriate class of biomarker for detecting early posttraumatic OA in young healthy individuals.

## Conclusions

In conclusion, we provide evidence for the first time that the serum level of Xylt1 rapidly increases during the early phase of OA progression in high bone formers. In addition, OA develops more rapidly in young healthy mice with high bone forming activity than in mice with high bone turnover. This is in agreement with the extensive epidemiological literature demonstrating that individuals with high systemic bone mass are at increased risk for OA [42]. Our data can be of great value in the screening and treatment of posttraumatic OA in young active individuals when sustained reloading of the previously injured joint is associated with increased bone synthesis. Altogether, knowledge of early molecular mechanisms involved between cartilage and adjacent tissues including subchondral bone during posttraumatic OA is essential to develop novel drug therapies effective at slowing disease progression and helping patients maintain an active and independent lifestyle for a longer period of time.

### Highlights

- The amount of soluble xylosyltransferases in peripheral blood can be used to determine the global rate of proteoglycan biosynthesis
- Xylosyltransferase 1 (Xylt1) level rapidly increases in the serum of C3H/HeJ mice following medial meniscectomy but remains steady in C57BL/6J
- Meniscectomy induces faster OA progression in the C3H/HeJ strain relative to the C57BL/6J strain
- Increase in serum Xylt1 positively correlates with cartilage damage at later time points in C3H/HeJ, the high bone former strain
- Xylt1 serum level may be used as a biomarker to predict OA in young patients who experienced joint trauma

## Supplementary Material

Refer to Web version on PubMed Central for supplementary material.

## Acknowledgments

This work was supported by an ARRA supplement to NIH P20-RR016458. The authors want to thank Mrs. Terry McLaughlin (AI DuPont Hospital for Children, Wilmington, DE) for assistance with knee histology and Ms. Jillian Hash and Mrs. Julie Hoffman (UD, Office Laboratory and Animal Medicine) for assistance with blood collection

and animal husbandry, respectively. We are also grateful to Dr. William Yang for valuable advice relative to mouse surgeries.

## Abbreviations

<b>BMD</b>	bone mineral density
<b>B6</b>	C57BL/6J
<b>C3H</b>	C3H/HeJ
<b>DMM</b>	destabilization of the medial meniscus
<b>GAG</b>	glycosaminoglycan
<b>OA</b>	osteoarthritis
<b>PG</b>	proteoglycan
<b>MX</b>	meniscectomy
<b>Xylt1</b>	xylosyltransferase 1

## References

1. Brown TD, Johnston RC, Saltzman CL, Marsh JL, Buckwalter JA. Posttraumatic osteoarthritis: a first estimate of incidence, prevalence, and burden of disease. *J Orthop Trauma*. 2006; 20:739–744. [PubMed: 17106388]
2. Glasson SS, Blanchet TJ, Morris EA. The surgical destabilization of the medial meniscus (DMM) model of osteoarthritis in the 129/SvEv mouse. *Osteoarthritis Cartilage*. 2007; 15:1061–1069. [PubMed: 17470400]
3. Welch ID, Cowan MF, Beier F, Underhill TM. The retinoic acid binding protein CRABP2 is increased in murine models of degenerative joint disease. *Arthritis Res Ther*. 2009; 11:R14. [PubMed: 19173746]
4. Kadri A, Funck-Brentano T, Lin H, Ea HK, Hannouche D, Marty C, Liote F, Geoffroy V, Cohen-Solal ME. Inhibition of bone resorption blunts osteoarthritis in mice with high bone remodelling. *Ann Rheum Dis*. 2010; 69:1533–1538. [PubMed: 20525838]
5. Mueller MB, Tuan RS. Anabolic/Catabolic balance in pathogenesis of osteoarthritis: identifying molecular targets. *Pm R*. 2011; 3:S3–S11. [PubMed: 21703577]
6. Billingham RC, Wu W, Ionescu M, Reiner A, Dahlberg L, Chen J, van Wart H, Poole AR. Comparison of the degradation of type II collagen and proteoglycan in nasal and articular cartilages induced by interleukin-1 and the selective inhibition of type II collagen cleavage by collagenase. *Arthritis Rheum*. 2000; 43:664–672. [PubMed: 10728761]
7. Billingham RC, Wu W, Ionescu M, Reiner A, Dahlberg L, Chen J, van Wart H, Poole AR. Enhanced cleavage of type II collagen by collagenases in osteoarthritic articular cartilage. *J Clin Invest*. 1997; 99:1534–1545. [PubMed: 9119997]
8. Garnero P, Ayrat X, Rousseau JC, Christgau S, Sandell LJ, Dougados M, Delmas PD. Uncoupling of type II collagen synthesis and degradation predicts progression of joint damage in patients with knee osteoarthritis. *Arthritis Rheum*. 2002; 46:2613–2624. [PubMed: 12384919]
9. Rizkalla G, Reiner A, Bogoch E, Poole AR. Studies of the articular cartilage proteoglycan aggrecan in health and osteoarthritis. Evidence for molecular heterogeneity and extensive molecular changes in disease. *J Clin Invest*. 1992; 90:2268–2277. [PubMed: 1281828]
10. Venkatesan N, Barre L, Magdalou J, Mainard D, Netter P, Fournel-Gigleux S, Ouzzine M. Modulation of xylosyltransferase I expression provides a mechanism regulating glycosaminoglycan chain synthesis during cartilage destruction and repair. *Faseb J*. 2009; 23:813–822. [PubMed: 19001053]
11. Prante C, Bieback K, Funke C, Schon S, Kern S, Kuhn J, Gastens M, Kleesiek K, Gotting C. The formation of extracellular matrix during chondrogenic differentiation of mesenchymal stem cells

- correlates with increased levels of xylosyltransferase I. *Stem Cells*. 2006; 24:2252–2261. [PubMed: 16778156]
12. Gotting C, Sollberg S, Kuhn J, Weilke C, Huerkamp C, Brinkmann T, Krieg T, Kleesiek K. Serum xylosyltransferase: a new biochemical marker of the sclerotic process in systemic sclerosis. *J Invest Dermatol*. 1999; 112:919–924. [PubMed: 10383739]
  13. Schon S, Huet G, Prante C, Muller S, Christ R, Hagen FW, Kuhn J, Kleesiek K, Gotting C. Mutational and functional analyses of xylosyltransferases and their implication in osteoarthritis. *Osteoarthritis Cartilage*. 2006; 14:442–448. [PubMed: 16376579]
  14. Sheng MH, Lau KH, Beamer WG, Baylink DJ, Wergedal JE. In vivo and in vitro evidence that the high osteoblastic activity in C3H/HeJ mice compared to C57BL/6J mice is intrinsic to bone cells. *Bone*. 2004; 35:711–719. [PubMed: 15336608]
  15. Kang, QK.; LaBreck, JC.; Gruber, HE.; An, YH. Histological Techniques for Decalcified Bone and Cartilage. In: An, YH.; Martin, KL., editors. *Handbook of Histology Methods for Bone and Cartilage*. Totowa: Humana Press Inc.; 2003. p. 209-219.
  16. Pritzker KP, Gay S, Jimenez SA, Ostergaard K, Pelletier JP, Revell PA, Salter D, van den Berg WB. Osteoarthritis cartilage histopathology: grading and staging. *Osteoarthritis Cartilage*. 2006; 14:13–29. [PubMed: 16242352]
  17. McDonald, JH. *Handbook of Biological Statistics*. Baltimore: Sparky House Publishing; 2009.
  18. Poole R, Blake S, Buschmann M, Goldring S, Laverty S, Lockwood S, Matyas J, McDougall J, Pritzker K, Rudolph K, van den Berg W, Yaksh T. Recommendations for the use of preclinical models in the study and treatment of osteoarthritis. *Osteoarthritis Cartilage*. 2010; 18:S10–S16. [PubMed: 20864015]
  19. Amblard D, Lafage-Proust MH, Chamson A, Rattner A, Collet P, Alexandre C, Vico L. Lower bone cellular activities in male and female mature C3H/HeJ mice are associated with higher bone mass and different pyridinium crosslink profiles compared to C57BL/6J mice. *J Bone Miner Metab*. 2003; 21:377–387. [PubMed: 14586794]
  20. Price C, Herman BC, Lufkin T, Goldman HM, Jepsen KJ. Genetic variation in bone growth patterns defines adult mouse bone fragility. *J Bone Miner Res*. 2005; 20:1983–1991. [PubMed: 16234972]
  21. Bergink AP, Uitterlinden AG, Van Leeuwen JP, Hofman A, Verhaar JA, Pols HA. Bone mineral density and vertebral fracture history are associated with incident and progressive radiographic knee osteoarthritis in elderly men and women: the Rotterdam Study. *Bone*. 2005; 37:446–456. [PubMed: 16027057]
  22. Dore D, Ding C, Jones G. A pilot study of the reproducibility and validity of measuring knee subchondral bone density in the tibia. *Osteoarthritis Cartilage*. 2008; 16:1539–1544. [PubMed: 18515160]
  23. Bruyere O, Dardenne C, Lejeune E, Zegels B, Pahaut A, Richey F, Seidel L, Ethgen O, Henrotin Y, Reginster JY. Subchondral tibial bone mineral density predicts future joint space narrowing at the medial femoro-tibial compartment in patients with knee osteoarthritis. *Bone*. 2003; 32:541–545. [PubMed: 12753870]
  24. Dieppe P, Cushnaghan J, Young P, Kirwan J. Prediction of the progression of joint space narrowing in osteoarthritis of the knee by bone scintigraphy. *Ann Rheum Dis*. 1993; 52:557–563. [PubMed: 8215615]
  25. Radin EL, Rose RM. Role of subchondral bone in the initiation and progression of cartilage damage. *Clin Orthop Relat Res*. 1986:34–40. [PubMed: 3780104]
  26. Amblard D, Lafage-Proust MH, Laib A, Thomas T, Rueggsegger P, Alexandre C, Vico L. Tail suspension induces bone loss in skeletally mature mice in the C57BL/6J strain but not in the C3H/HeJ strain. *J Bone Miner Res*. 2003; 18:561–569. [PubMed: 12619942]
  27. Robling AG, Turner CH. Mechanotransduction in bone: genetic effects on mechanosensitivity in mice. *Bone*. 2002; 31:562–569. [PubMed: 12477569]
  28. Goldring MB, Goldring SR. Articular cartilage and subchondral bone in the pathogenesis of osteoarthritis. *Ann N Y Acad Sci*. 2010; 1192:230–237. [PubMed: 20392241]

29. Muller B, Prante C, Gastens M, Kuhn J, Kleesiek K, Gotting C. Increased levels of xylosyltransferase I correlate with the mineralization of the extracellular matrix during osteogenic differentiation of mesenchymal stem cells. *Matrix Biol.* 2008; 27:139–149. [PubMed: 17980567]
30. Prante C, Kuhn J, Kleesiek K, Gotting C. High xylosyltransferase activity in children and during mineralization of osteoblast-like SAOS-2 cells. *Glycoconj J.* 2009; 26:219–227. [PubMed: 18763033]
31. Nagase H, Kashiwagi M. Aggrecanases and cartilage matrix degradation. *Arthritis Res Ther.* 2003; 5:94–103. [PubMed: 12718749]
32. Frisbie DD, Al-Sobayil F, Billingham RC, Kawcak CE, McIlwraith CW. Changes in synovial fluid and serum biomarkers with exercise and early osteoarthritis in horses. *Osteoarthritis Cartilage.* 2008; 16:1196–1204. [PubMed: 18442931]
33. Catterall JB, Stabler TV, Flannery CR, Kraus VB. Changes in serum and synovial fluid biomarkers after acute injury (NCT00332254). *Arthritis Res Ther.* 2010; 12:R229. [PubMed: 21194441]
34. Svoboda, S.; Harvey, T.; Brechue, W.; Owens, B.; Cameron, K. Abstract OA Biomarker Global Initiative Workshop II. Atlanta: OARSI; 2010. Changes in serum biomarkers of cartilage turnover following ACL reconstruction.
35. Clements KM, Price JS, Chambers MG, Visco DM, Poole AR, Mason RM. Gene deletion of either interleukin-1beta, interleukin-1beta-converting enzyme, inducible nitric oxide synthase, or stromelysin 1 accelerates the development of knee osteoarthritis in mice after surgical transection of the medial collateral ligament and partial medial meniscectomy. *Arthritis Rheum.* 2003; 48:3452–3463. [PubMed: 14673996]
36. Schon S, Prante C, Bahr C, Kuhn J, Kleesiek K, Gotting C. Cloning and recombinant expression of active full-length xylosyltransferase I (XT-I) and characterization of subcellular localization of XT-I and XT-II. *J Biol Chem.* 2006; 281:14224–14231. [PubMed: 16569644]
37. Mitton E, Gohr CM, McNally MT, Rosenthal AK. Articular cartilage vesicles contain RNA. *Biochem Biophys Res Commun.* 2009; 388:533–538. [PubMed: 19679100]
38. Fritton JC, Myers ER, Wright TM, van der Meulen MC. Loading induces site-specific increases in mineral content assessed by microcomputed tomography of the mouse tibia. *Bone.* 2005; 36:1030–1038. [PubMed: 15878316]
39. Hunter DJ, Lavalley M, Li J, Bauer DC, Nevitt M, DeGroot J, Poole R, Eyre D, Guermazi A, Gale D, Totterman S, Felson DT. Biochemical markers of bone turnover and their association with bone marrow lesions. *Arthritis Res Ther.* 2008; 10:R102. [PubMed: 18759975]
40. Kokebie R, Aggarwal R, Lidder S, Hakimiyani AA, Rueger DC, Block JA, Chubinskaya S. The role of synovial fluid markers of catabolism and anabolism in osteoarthritis, rheumatoid arthritis and asymptomatic organ donors. *Arthritis Res Ther.* 2011; 13:R50. [PubMed: 21435227]
41. Richman C, Kutilek S, Miyakoshi N, Srivastava AK, Beamer WG, Donahue LR, Rosen CJ, Wergedal JE, Baylink DJ, Mohan S. Postnatal and pubertal skeletal changes contribute predominantly to the differences in peak bone density between C3H/HeJ and C57BL/6J mice. *J Bone Miner Res.* 2001; 16:386–397. [PubMed: 11204439]
42. Goldring SR, Goldring MB. Bone and cartilage in osteoarthritis: is what's best for one good or bad for the other? *Arthritis Res Ther.* 2010; 12:143. [PubMed: 21044355]



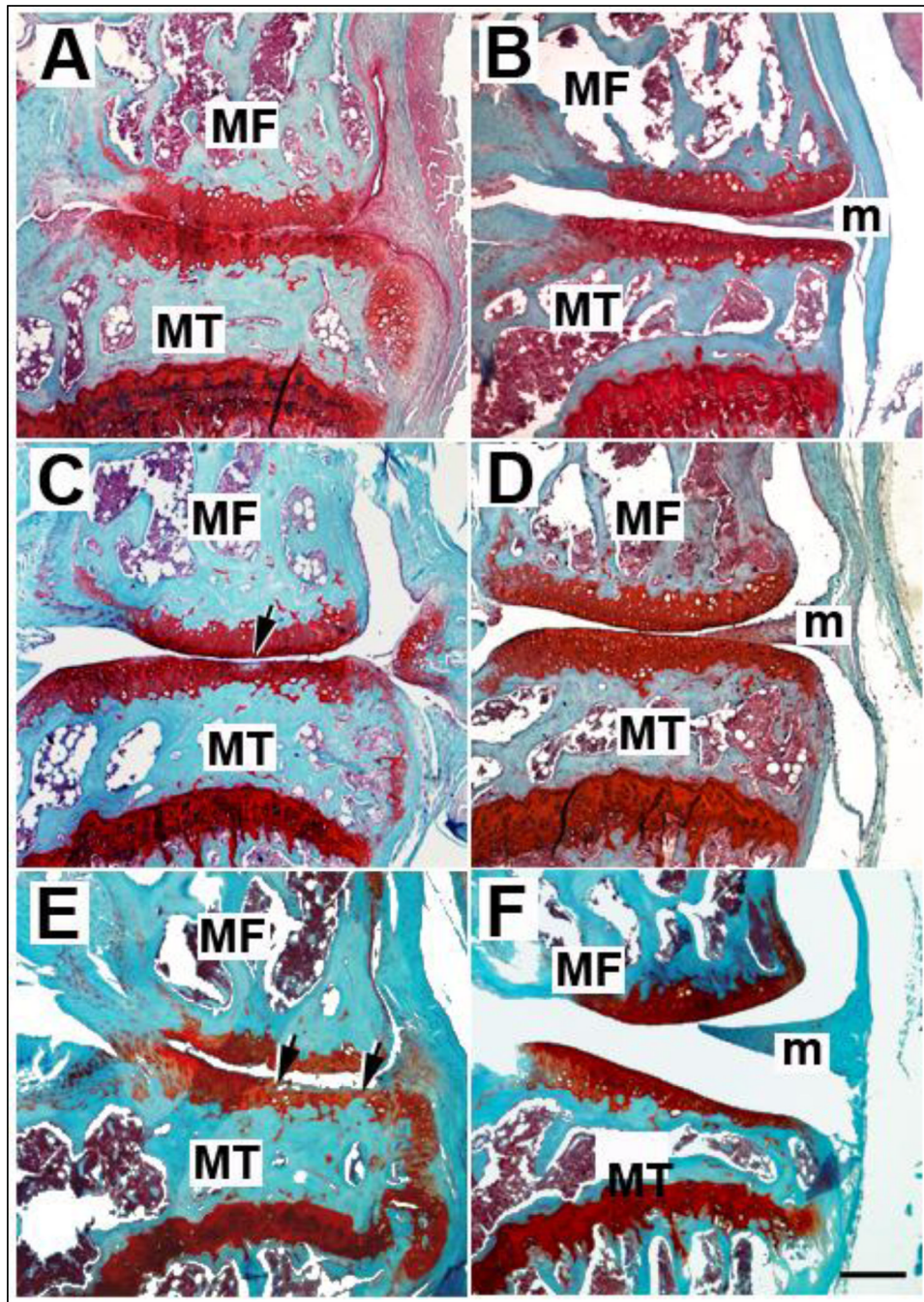


**Fig. 1.** Representative histological images of B6 mouse knees processed 1 (A–B, n=4), 2 (C–D, n=5), or 3.5 (E–F, n=8) months following MNX (A, C, E) or sham (B, D, F) surgeries. Safranin-O staining revealed OA lesions in MNX knees and cartilage damage located at the tibial surface is indicated by arrows. No damage of articular cartilage is observed for control shams at identical time points. MT, medial tibia; MF, medial femur; m, meniscus. Magnification bar = 200 $\mu$ m.



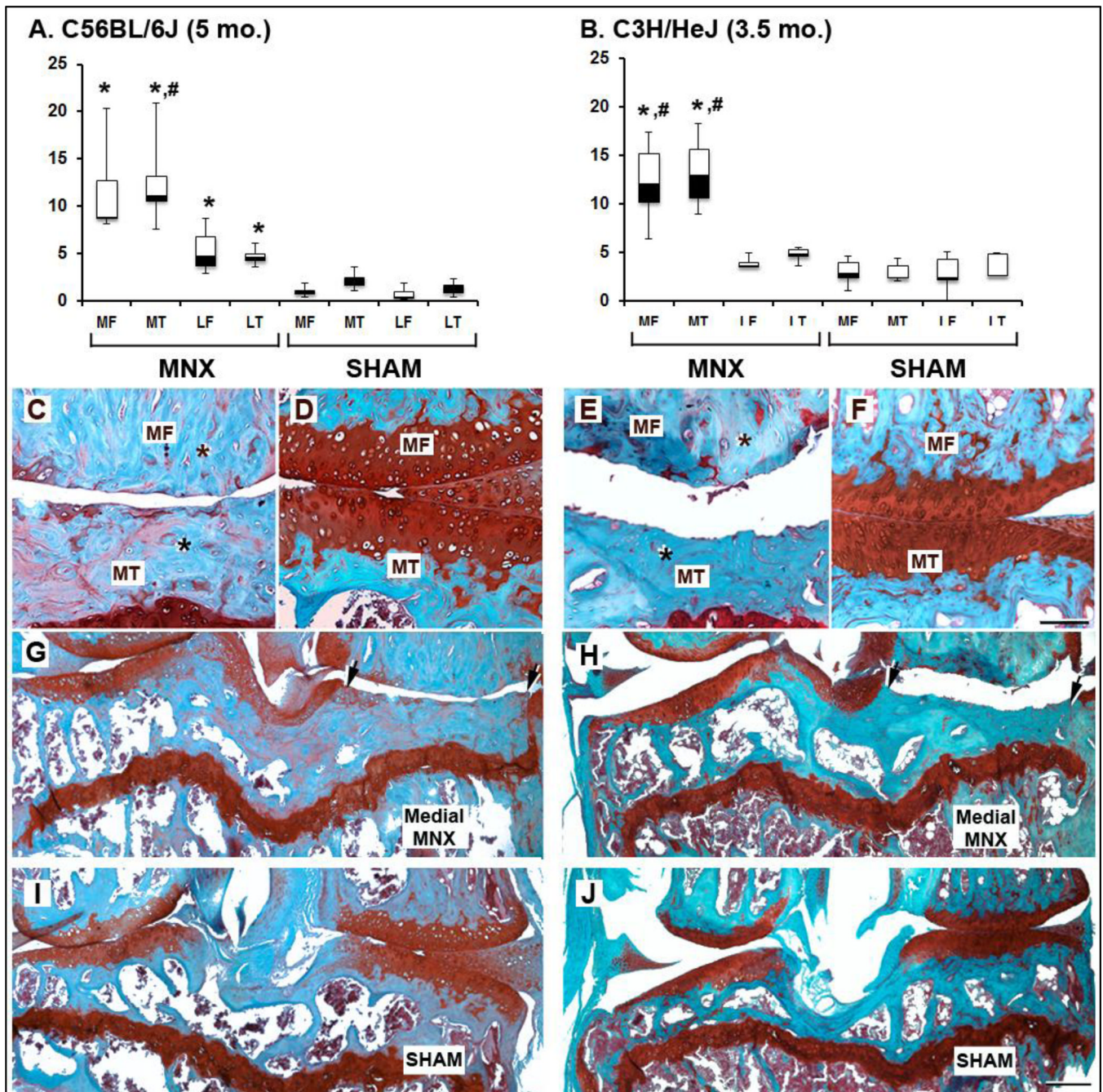


**Fig. 2.** Comparative histology of full-thickness cartilage damage in B6 and C3H mouse strains. Box and whisker plots showing the median (central line), 25–75 percentile (boxes) and the entire range of scores (whiskers) obtained 3.5 (B) or 5 (A) months after MNX or sham surgeries for C3H or B6, respectively ( $n=5/\text{group}$ ). \* indicates significant changes ( $p<0.0125$ ) when MNX scores were compared to sham scores in the same knee compartments. # indicates significant changes ( $p<0.0125$ ) when medial and lateral compartments of the same knee were compared. No statistical difference is seen between the medial and lateral compartments of sham scores in either B6 or C3H mice. MT, medial tibia; MF, medial femur; m, meniscus. Asterisks in subchondral bone indicate a decrease in bone marrow

space following partial medial MNX (C, E, G, H) relative to control sham (D, F, I, J) knees. Magnification bars in D = 100 $\mu$ m (A–D), and in J = 200 $\mu$ m (G–J).

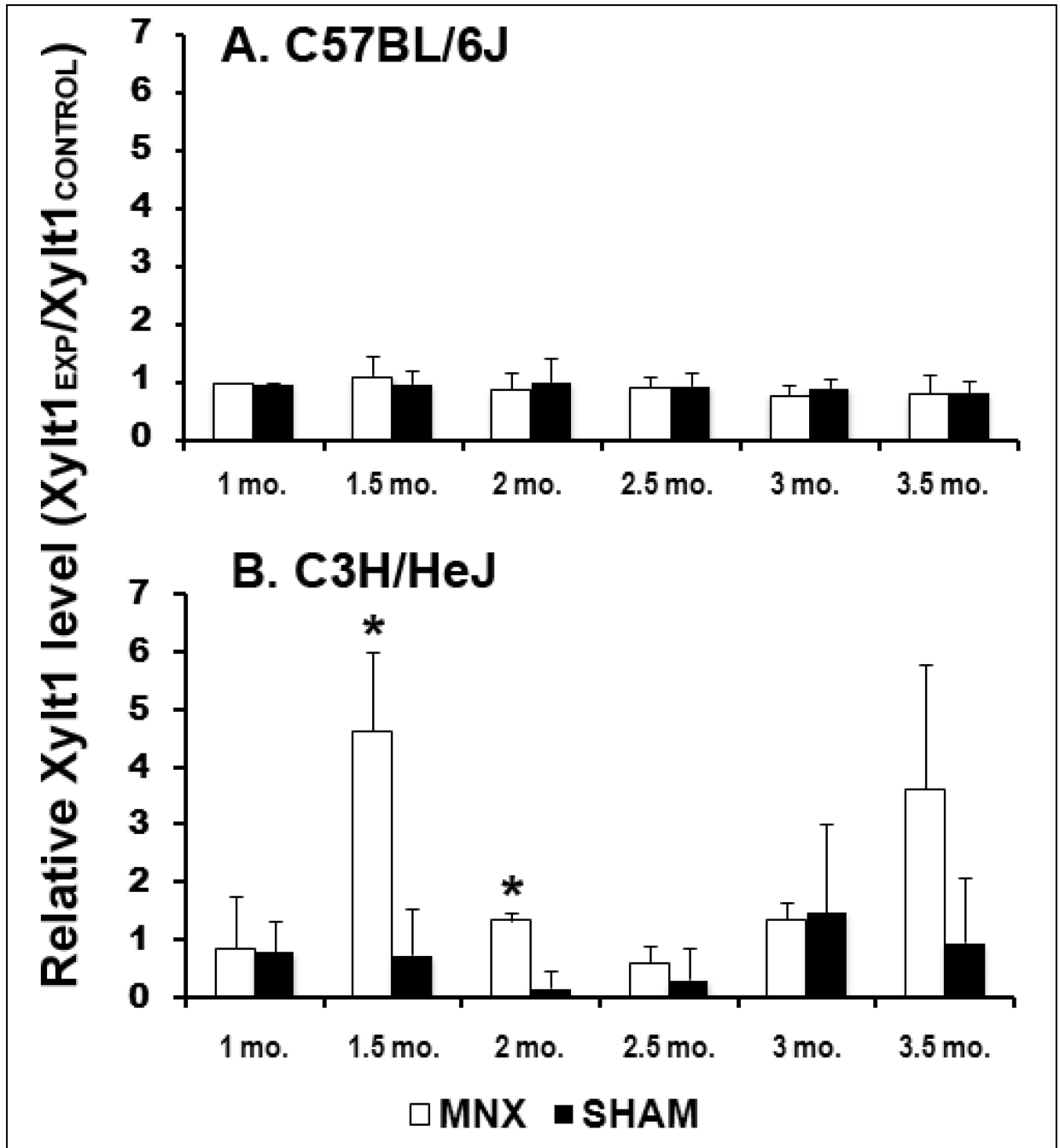


**Fig. 3.** Evolution of serum Xylt 1 levels in MNX and sham-operated B6 (A) and C3H (B) mice (n=5 per group). \* indicates significant changes ( $p < 0.005$ ) in MNX vs. sham-operated C3H at either 1.5 or 2 months post-surgery. A trend increase is observed at 3.5 months in MNX relative to sham C3H ( $P = 0.08$ ). No significant difference in Xylt 1 levels was observed between MNX and sham B6 mice at all time points examined. Data are shown as the ratio of the mean densitometric value obtained for Xylt1 in the experimental group over the densitometric value of the loading control ( $Xylt1_{EXP}/Xylt1_{CONTROL}$ ) and error bars represent standard deviations.

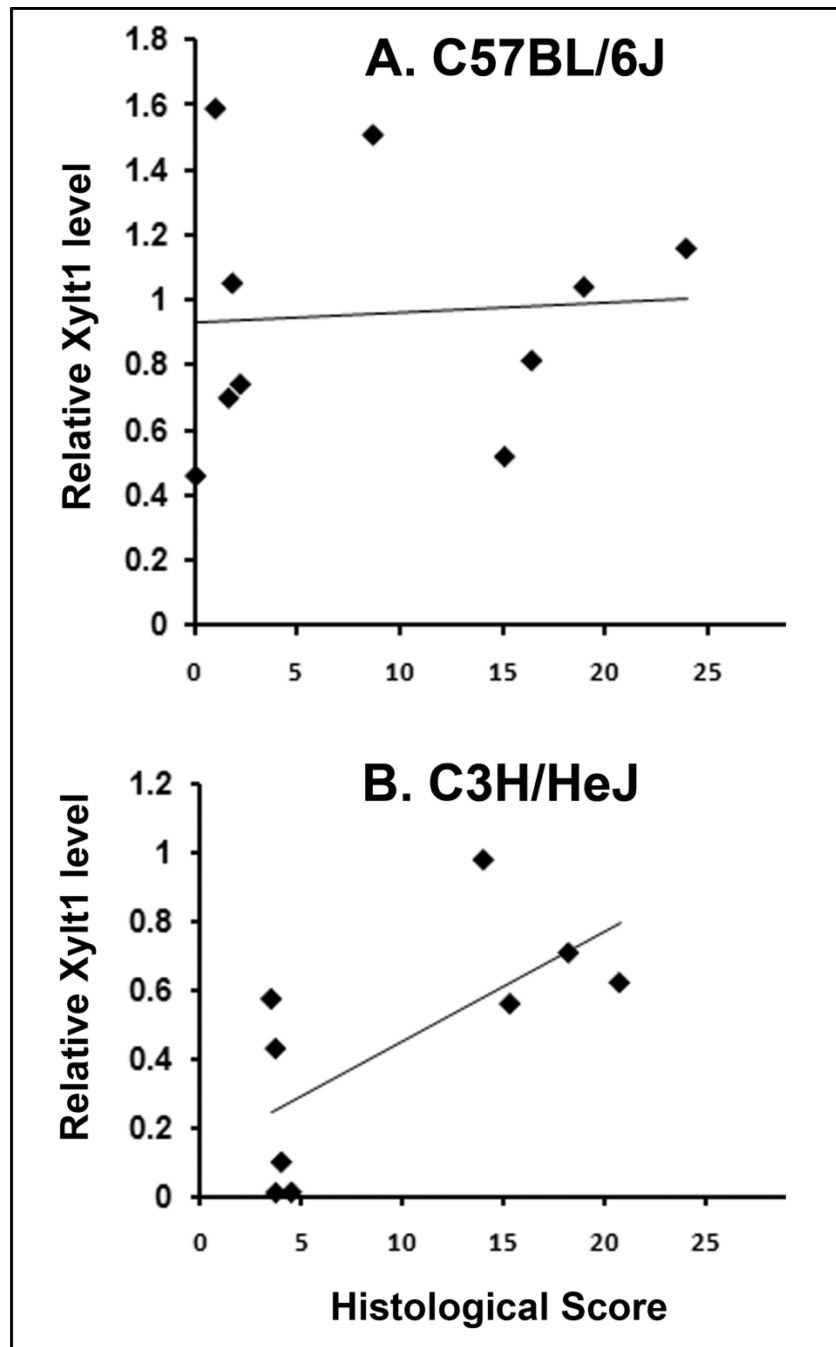


**Fig. 4.** Correlations between Xylt 1 levels at 2 months post-surgery and medial histomorphological knee scores in B6 (A) and C3H (B) mice. N = 9.

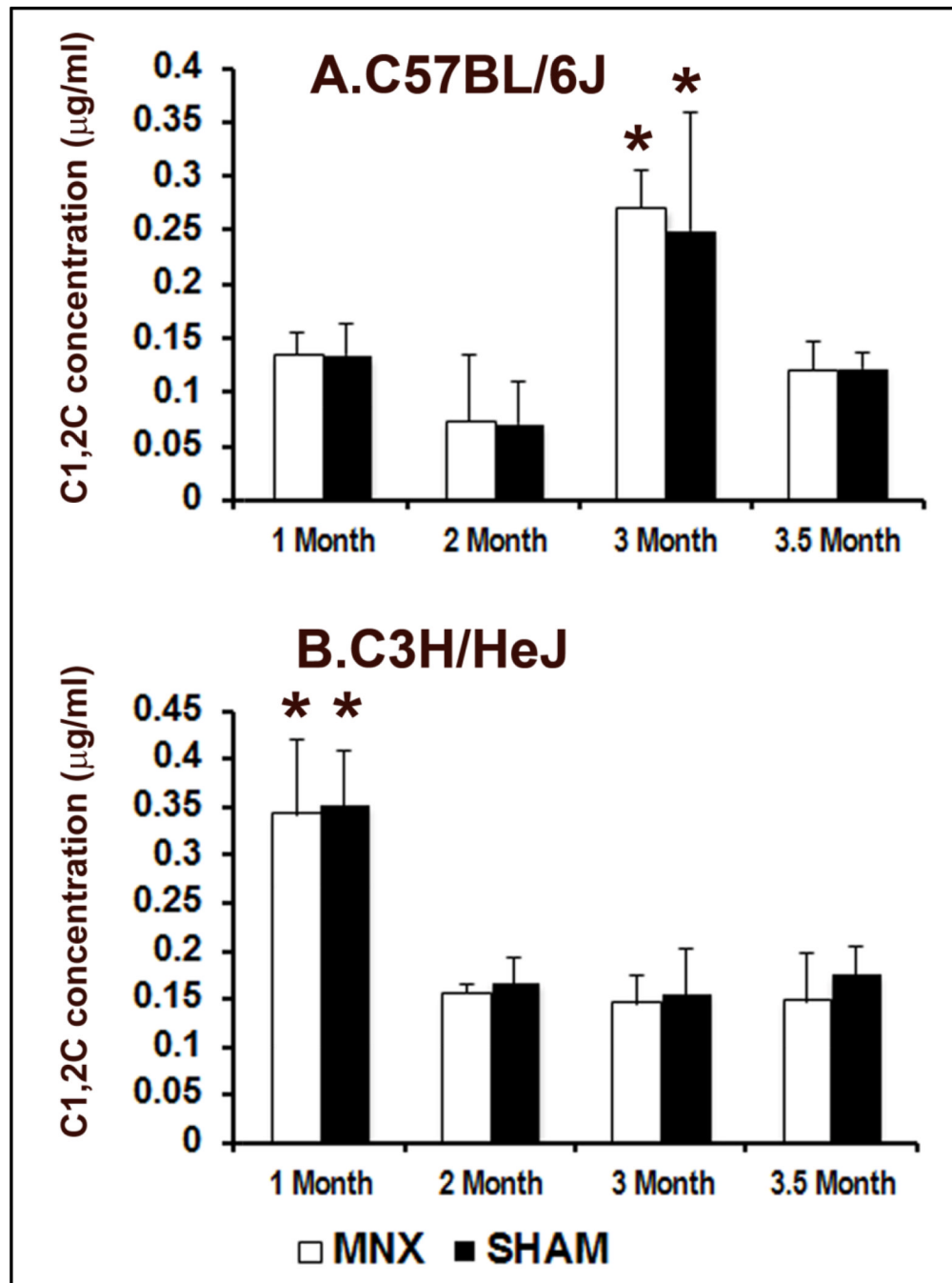


**Fig. 5.** Evolution of C1,2C levels in MNX and sham-operated B6 (A) and C3H (B) mice (n=5 per group). \* indicates significant difference in the level of C1,2C between different time points. No significant change is seen between MNX and sham surgeries at identical time points within an individual mouse strain. Data are shown as mean values and error bars represent standard deviations.



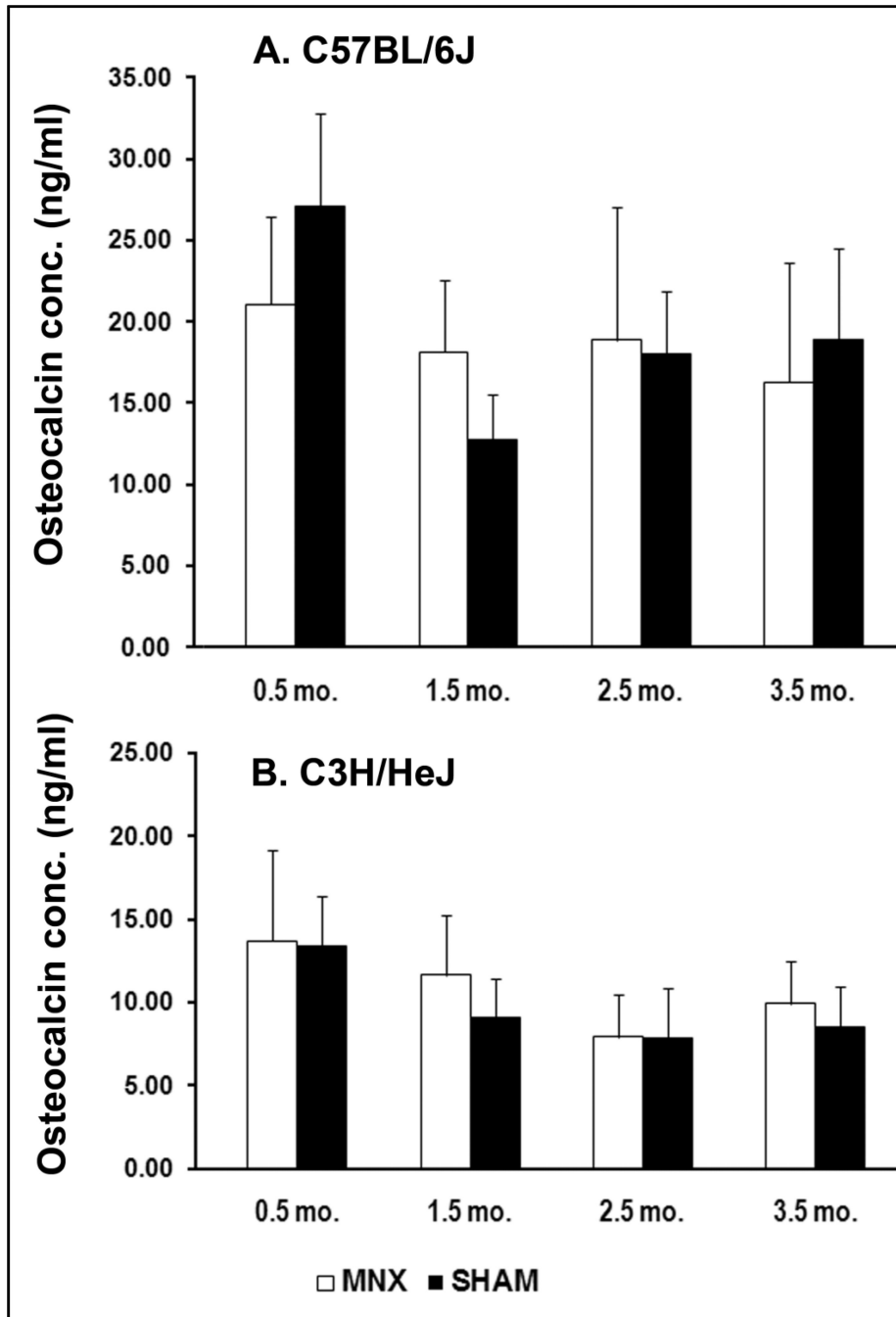


**Fig. 6.** Evolution of osteocalcin concentrations in MNX and sham-operated B6 (A) and C3H (B) mice (n=5 per group). No significant change is seen between MNX and sham surgeries at identical time points within an individual mouse strain. Data are shown as mean values and error bars represent standard deviations.